Molecular Pharmacology Fast Forward. Published on March 7, 2013 as doi: 10.1124/mol.112.084368
This article has not been copyedited and formatted. The final version may differ from this version.

MOL# 84368

A Newly Synthesized Sinapic Acid Derivative Inhibits Endothelial Activation *In Vitro* and *In Vivo*

Xiaoyun Zeng, Jinhong Zheng, Chenglai Fu, Hang Su, Xiaoli Sun, Xuesi Zhang, Yingjian Hou, and Yi Zhu

Cardiovascular Research Center, Shantou University Medical College, Shantou, Guangdong, 515041, China (XZ, HS, XZ, YZ); Department of Chemistry, Shantou University Medical College, Shantou, Guangdong, 515041, China (JZ); Department of Physiology and Pathophysiology, Peking University Health Sciences Center, Beijing, 100191, China (CF, XS, YH); Department of Physiology and Pathophysiology, Tianjin Medical University, Tianjin, 300070, China (YZ)

Footnote

Molecular Pharmacology Fast Forward. Published on March 7, 2013 as DOI: 10.1124/mol.112.084368
This article has not been copyedited and formatted. The final version may differ from this version.

Running Title：*Zeng et al: Sinapic Acid Derivative Inhibits EC Activation*

Corresponding author: Yi Zhu, MD, Department of Physiology and Pathophysiology, Tianjin Medical University, 20 Qixiangtai Road, Tianjin, 300070, China. Tel.: (8622) 8333-6665; Fax: (8622) 8333-6660; E-mail: zhuyi@tmu.edu.cn

Number of text pages	29
Tables	1
Figures	6
References	43
Abstract Word Count	241
Introduction Word Count	709
Discussion Word Count	743

List of Abbreviations

SA	sinapic acid
SA9	1-acetyl-sinapic acyl-4-(3'-Chlorine-) benzylpiperazine
ECs	endothelial cells
HUVECs	human umbilical vein endothelial cells
ROS	reactive oxygen species
ICAM-1	intercellular adhesion molecule 1
VCAM-1	vascular cell adhesion molecule 1
COX-2	Cyclooxygenase-2
TNF-α	tumor necrosis factor-alpha

Molecular Pharmacology Fast Forward. Published on March 7, 2013 as DOI: 10.1124/mol.112.084368
This article has not been copyedited and formatted. The final version may differ from this version.

LPS	lipopolysaccharide

Abstract

Inhibition of oxidative stress and inflammation in vascular endothelial cells (ECs) may represent a new therapeutic strategy against endothelial activation. Sinapic acid (SA), a phenylpropanoid compound, is found in natural herbs and high-bran cereals and has moderate antioxidant activity. We aimed to develop new SA agents with the properties of antioxidation and blocking EC activation for possible therapy of cardiovascular disease. We designed and synthesized 10 SA derivatives according to their chemical structures. Preliminary screening of the compounds involved scavenging hydroxyl radicals and DPPH•, croton oil-induced ear edema in mice and analysis of the mRNA expression of adhesion molecules in ECs. SA9 had the strongest antioxidant and anti-inflammatory activities both *in vitro* and *in vivo*. Thus, the effect of SA9 was further studied. SA9 inhibited tumor necrosis factor α-induced upregulation of adhesion molecules in ECs at both mRNA and protein levels, as well as the consequent monocyte adhesion to ECs. *In vivo*, result of *en face* immunostaining showed that SA9 reduced lipopolysaccharide-induced expression of intercellular adhesion molecule 1in mouse aortic intima. To study the molerular mechanism, Results from luciferase assay, nuclear translocation of NF-κB and western blot indicated that the mechanism of the anti-inflammatory effects of SA9 might be suppression of intracellular generation of ROS and inhibition of NF-κB activation in ECs. SA9 is a prototype of a novel class of antioxidant with anti-inflammatory effects in ECs. It may represent a new therapeutic approach for preventing endothelial activation in cardiovascular disorders.

Molecular Pharmacology Fast Forward. Published on March 7, 2013 as DOI: 10.1124/mol.112.084368
This article has not been copyedited and formatted. The final version may differ from this version.

Introduction

In response to various inflammatory stimuli, endothelial cells (ECs) become activated, which leads to impaired endothelium-dependent vasodilation, inadequate perfusion, vascular leakage, and inflammation. Abnormalities occur in endothelial interactions with leukocytes, platelets and regulatory substances (Anderson, 1999; Pober et al., 2009). EC activation plays a key role in inflammation, thrombosis and atherogenesis. Activated ECs express and activate specific adhesion molecules, such as vascular cell adhesion molecule 1 (VCAM-1) and intercellular adhesion molecule 1 (ICAM-1), which then recruit leukocytes such as monocytes, lymphocytes, or neutrophils (Butcher, 1991). VCAM-1 and ICAM-1 have an important role in endothelial dysfunction and vascular lesion development. The recruitment of leukocytes from circulating blood is crucial in the inflammatory reaction and is a multistep process: sequential capture, rolling along and firm adhesion to the microvascular endothelium, and transmigration through the vessel wall and further migration in extravascular tissue. All these steps are orchestrated by cell-adhesion molecules on both leukocytes and endothelial cells, and different subsets of adhesion molecules are responsible for the different steps in extravasation. The expression of adhesion molecules in the large-vessel endothelium is considered a key factor in the development of atherosclerotic lesions. Upregulation of adhesion molecules with many other genes is considered to indicate EC activation.

Many endothelial functions are sensitive to the presence of reactive oxygen species (ROS) and subsequent oxidative stress (Davignon and Ganz, 2004). Pathologic processes fundamental to the development and progression of endothelial dysfunction such as the oxidation of low-density lipoprotein, loss of bioavailable nitric oxide, and the vascular inflammatory response are all modulated by oxidant stress (Fenster et al., 2003). Inflammatory cytokines induce EC activation by increasing ROS generation and enhancing the activity and expression of oxidative stress markers such as NF-κB and ICAM-1 and

Molecular Pharmacology Fast Forward. Published on March 7, 2013 as DOI: 10.1124/mol.112.084368
This article has not been copyedited and formatted. The final version may differ from this version.

VCAM-1 (Alom-Ruiz et al., 2008; Borel et al., 2009; Wagener et al., 1997). Tumor necrosis factor-α (TNF-α) and lipopolysaccharide (LPS) increase the expression of ICAM-1 and VCAM-1 through an NF-κB–dependent redox-sensitive mechanism in ECs (Alom-Ruiz et al., 2008; Kim et al., 2011). Thus, modulation of these processes -- elimination of ROS, inhibiting the activation of NF-κB and monocyte adherence -- assumes great significance in preventing and treating EC dysfunction. Antioxidants may be an attractive therapeutic strategy to reduce endothelial dysfunction and prevent and treat cardiovascular disease (Bonetti et al., 2003; Versari et al., 2009).

Exogenous antioxidants may protect endothelial function by modulating EC-dependent vasodilation responses, homeostatic EC–monocyte interactions, the balance between pro- and anti-thrombotic properties, and vascular apoptotic responses (Pratico, 2005). A number of preclinical lines of evidence support this concept, and despite many studies suggesting a beneficial impact of antioxidant drugs on endothelial function, studies of the effects of classical antioxidants such as vitamin C, vitamin E, or folic acid combined with vitamin E have been disappointing (Munzel et al., 2010). In contrast, substances such as statins, angiotensin-converting enzyme inhibitors, or AT1-receptor blockers, which have indirect antioxidant properties mediated by the stimulation of nitric oxide production and simultaneous inhibition of superoxide production, could improve vascular function in pre-clinical and clinical studies and reduce the incidence of cardiovascular events in patients with cardiovascular disease (Anderson, 1999; Munzel et al., 2010; Shindel et al., 2008). Oxidative stress remains an attractive target for cardiovascular prevention and therapy, and developing novel antioxidants from natural compounds is an interesting research direction.

One class of antioxidants is phenolic acids, many of which are natural compounds. Sinapic acid (SA) is a major component of traditional Chinese medicine found in *Ligusticum chuaxiong Hort, Descurainia sophia, and Cimicifuga foetida L.* SA retains its hydroxyl in the

Molecular Pharmacology Fast Forward. Published on March 7, 2013 as DOI: 10.1124/mol.112.084368
This article has not been copyedited and formatted. The final version may differ from this version.

presence of antioxidants. As well, the carboxylic acids in SA can be converted to amides and benzyl-substituted piperazine to increase its lipophilicity so that it may more easily pass through a cellular plasma membrane. The SA piperazine, a novel pharmacophore, may increase new pharmacological activity. Therefore, transforming the structure of SA may be an effective way to develop new compounds with pharmacological activity.

In this study, we designed and synthesized a series of 1-erucic acyl-4-benzyl piprazine derivatives of SA (SA1~SA10). We tested the antioxidant ability of the most active compound [1-acetyl-sinapic acyl-4-(3'-chlorine-) benzyl piperazine (SA9)] on EC activation *in vitro* and *in vivo* and investigated the underlying mechanism of the protective effects in TNF-α–induced endothelial activation.

Molecular Pharmacology Fast Forward. Published on March 7, 2013 as DOI: 10.1124/mol.112.084368
This article has not been copyedited and formatted. The final version may differ from this version.

Materials and Methods

Reagents, antibodies and EC culture

Antibodies for VCAM-1, ICAM-1, JNK1, p65, phosphorylated-ERK (p-ERK) and total ERK were from Santa Cruz Biotechnology (Santa Cruz, CA). Antibodies for anti-IκBα, anti-p-IκBα and anti-p-SAPK/JNK were from Cell Signaling (Danvers, MA, USA). Anti-ICAM-1 for immunostaining was from R&D Systems. Phorbol 12-myristate 13-acetate (PMA), LPS, TNF-α, dihydroethidium (DHE), bisbenzimide H 33258, Hoechst 33342, 2,2-diphenyl-1-picrylhydrazyl (DPPH•), 2',7'-dichlorfluorescein-diacetate (DCFH-DA), N-acetyl-L-cysteine (NAC) and Dibenziodolium chloride (DPI) were from Sigma (St. Louis, MO). 2',7' - bis - (2 - carboxyethyl) - 5 - (and - 6) - carboxyfluorescein (BCECF) was from Invitrogen (Carlsbad, CA). Cell culture reagents and other reagents were from Hyclone, Gibco, or Sigma.

Human umbilical vein ECs (HUVECs) were isolated and cultured as previously described (Zhu et al., 2008). The investigation conforms to the principles in the Declaration of Helsinki for use of human tissue. All experiments were performed with HUVECs up to passage 6 and cultured to confluence before treatment.

DPPH• radical scavenging assay

Free radical scavenging activities were measured by use of the stable DPPH radical (DPPH•) as described (Lum and Roebuck, 2001) with modification. Briefly, 65 μM solution of DPPH• in ethanol was added to samples at different concentrations (0.05–6.0 μM). The mixture was vortexed at room temperature for 20 min in dark, and the absorbance was measured at 517 nm. The capability to scavenge DPPH• was calculated by the following equation: *% radical scavening capacity* = $[(A_0 - A_1)/A_0] \times 100$, where A_0 is the absorbance of the control reaction and A_1 is the absorbance in the presence of sample, corrected for the

Molecular Pharmacology Fast Forward. Published on March 7, 2013 as DOI: 10.1124/mol.112.084368
This article has not been copyedited and formatted. The final version may differ from this version.

absorbance of sample itself. The scavenging activity was expressed as the EC_{50} value (μM). Linear regression equations of absorbance against concentrations were determined by measuring the absorbance of 14 different concentrations of DPPH (6.5×10^{-4} M) stock solution: A (517 nm) = 7.9989C + 0.0265 (R^2= 0. 999).

Hydroxyl radical scavenging assay

Hydroxyl radical scavenging capacity was determined as described (Ming et al., 1996). The reaction mixture contained orthophenanthroline (75 μM), acetic acid (50 μM, pH 3.0), iron(II) sulfate (75 μM), 0.1% H_2O_2 and concentrations (0.04~1.20 mM) of the test samples or the reference compound, except for SA6 and SA10 (0.02~0.78 mM). After incubation for 1 hr at 37°C, the absorbance was measured at 536 nm against an appropriate blank solution. The capacity to scavenge hydroxyl radicals was calculated as follows: *% radical scavening capacity* = $[(A_0 - A_1)/A_2] \times 100$, where A_0 is the absorbance in the presence of the sample, A_1 is the absorbance of the control without a sample, and A_2 is the absorbance of the control without a sample and H_2O_2.

Toxicity assay for SAs in HUVECs

The effect of SA1~SA10 on cell number was analyzed by MTT assay for cell toxicity as described (Zhang et al., 2006). The corrected absorbance of each sample was calculated by comparison with the untreated control.

Quantitative real-time RT-PCR (qRT-PCR)

qRT-PCR was performed as we previously described (Zhang et al., 2010). Total cellular or tissue RNA was isolated by the Trizol reagent method (Invitrogen) and reverse transcribed by use of the First Strand cDNA Synthesis kit (Thermo Scientific, Rockford, IL). The amplification reactions were in a volume of 20 μl consisting of synthesized cDNA, primers and EasyTaq PCR Mix (Transgen Biotech, Beijing). Eva Green I fluorescence (Invitrogen) was used to monitor amplification of DNA by the MX3000P qPCR detection system

Molecular Pharmacology Fast Forward. Published on March 7, 2013 as DOI: 10.1124/mol.112.084368
This article has not been copyedited and formatted. The final version may differ from this version.

(Stratagene, Santa Clara, CA). Fold change in mRNA concentration was calculated by the comparative CT method. Gene expression was normalized to that of the housekeeping gene β-actin. The forward and reverse PCR primers were for GAPDH, 5'-gagtcaacggatttggtcgt-3', 3'-ttgattttggagggatctcg-5'; ICAM-1, 5'-tggagtccagtacacggtga-3', 5'-catagagaccccgttgccta-3'; VCAM-1, 5'-taaaatgcctgggaagatgg-3', 5'-ctgtggtgctgcaagtcaat-3'; and cyclooxygenase 2 (COX-2), 5'-tgaaacccactccaaacaca -3', 5'-gagaaggcttcccagctttt-3.

Western blot analysis

Protein isolation and western blot analysis were as described (Fu et al., 2011) with anti-ICAM-1, anti-VCAM-1, anti-JNK1, anti-p-ERK, anti-ERK, anti-IκBα, anti-p-IκBα and anti-p-SAPK/JNK antibodies following standard protocols. Anti-β-actin (Bioss, Beijing) was used as a loading control. The protein bands were visualized by enhanced chemiluminescence (Amersham, Arlington Heights, IL), and band densities were quantified by use of Scion Image software (Scion, Frederick, MD).

Immunofluorescence analysis

Subconfluent HUVECs grown on coverslips were treated as indicated. The cells were fixed with 4% paraformaldehyde and immunostained with anti-p65 primary antibody, then anti-rabbit FITC-conjugated secondary antibody. Nuclei were stained with Hoechst 33342. Staining was observed under a confocal microscope.

Detection of superoxide anion and ROS *in situ*

Generation of superoxide anion in HUVECs was measured by DHE staining and fluorescence microscopy as described (Lefevre et al., 2007). Briefly, serum-free medium containing DHE (5 μM) was applied onto each plate of cells for 20 min and washed. Then, cells were treated with 10 $ng \cdot ml^{-1}$ TNF-α with or without 1 mM NAC, 20 μM DPI and 1 μM SA9, respectively for 20 min and examined under an inverted fluorescence microscopy. DHE

Molecular Pharmacology Fast Forward. Published on March 7, 2013 as DOI: 10.1124/mol.112.084368
This article has not been copyedited and formatted. The final version may differ from this version.

fluorescence intensity was measured by use of a fluorescence microplate reader (BioTek, Gen5) at 485/620 nm. Generation of ROS in HUVECs was measured by DCFH-DA staining by use of a fluorescence microplate reader (BioTek, Gen5) with wavelength 485/528 nm and fluorescence microscopy (Corda et al., 2001). Generations of superoxide anion and ROS in mice ears were measured by DHE and DCFH-DA staining as described (Robert P. et al., 2008). Generation of superoxide anion and ROS in mouse ears was measured by DHE and DCFH-DA staining, separately. Briefly, frozen sections were then incubated with 5 μM DHE or 10 μM DCFH-DA in PBS at room temperature in the dark for 30 min, then coverslipped with fluorescent mounting medium. Staining was observed with use of the AxioVision Imaging System (Carl Zeiss MicroImaging GmbH 07740 Jena, Deutschland).

Cell adhesion assay

Cell adhesion assay was performed as described (Fu et al., 2010a) with modification. Briefly, HUVECs were pretreated with 1 μM SA9 for 30 min, then 10 $ng \cdot ml^{-1}$ TNF-α for 8 hr. THP-1 cells were stimulated with or without 5 nM PMA for 24 hr, then labeled with fluorescence dye (BCECF). The treated HUVECs and THP-1 cells were co-incubated for 15 min. Non-adhering cells were washed off, and adhered THP-1 cells were counted under a fluorescence microscope.

Luciferase activity assay

For transient transfection, 5×NF-κB/Luc plasmid was transfected into Hy926 cells by use of the jetPEI method (PolyPlus, Illkirch, France) 24 hr before further treatment ((Dang et al., 2009). Cells were then subjected to various treatments as indicated, then were lysed to measure luciferase and β-galactosidase reporter activities. Luciferase activity was normalized to internal control β-galactosidase activity.

Animal care and experimental procedure

The investigation conformed to the Guide for the Care and Use of Laboratory Animals

Molecular Pharmacology Fast Forward. Published on March 7, 2013 as DOI: 10.1124/mol.112.084368
This article has not been copyedited and formatted. The final version may differ from this version.

published by the US National Institutes of Health (NIH Publication No. 85–23, revised 1996). C57B mice were from the Peking University Health Science Center. BALB/c mice were from the Guangzhou First Military Medical University Animal Center (license no.: SCXK (Guangdong) 2006-0015, 2006B008). All experimental protocols were approved by the University Institutional Animal Care and Use Committee.

The model of croton oil-induced ear edema and inflammation was as described (Conforti et al., 1991). BALB/c mice (male, 25 ~ 30 g) were randomly divided into 4 groups (n=8 each). The non-steroidal anti-inflammatory drug ibuprofen was used as a reference. The test sample was orally administered (0.2 ml·10g^{-1} body weight) 60 min before croton oil-induced ear edema. Croton oil was applied (1%, 50 μL per mouse) topically on the right ear pinna of mice, and the left pinna was used as control. The mice were euthanized 4 hr later; both ears were removed, and circular sections (8 mm diameter) of ears were punched out with the use of a cork borer and weighed. Edema was quantified as the difference in weight between the 2 ear pinnas. Anti-inflammatory activity was evaluated as percentage inhibition in the treated animals relative to controls as follows: inhibition (%) = [(Rc-Lt)/Rc]×100%, where Rc is mean edema of control mice and Lt mean edema of treated mice (Olajide et al., 2000). Ear thickness was analyzed by use of ImageJ. Frozen sections of mice ears were prepared for DHE, DCFH and hematoxylin and eosin (H&E) staining.

For *en face* immunostaining of aortas, C57B mice were fed 50 mg·kg^{-1} SA9 for 1 hr, then inflammation was induced by intraperitoneal injection of LPS (10 mg·kg^{-1} body weight) for 8 hr before mice were euthanized (Garrean S, 2006). Immunostaining for ICAM-1 in aortic intima of mice was as described (Verna et al., 2006). After perfusion fixation and dissection, aortas were incubated with 20% goat serum, then mouse anti-ICAM-1 antibody at 4°C overnight. Secondary antibody was Cy3-labeled goat anti-mouse antibody.

Molecular Pharmacology Fast Forward. Published on March 7, 2013 as DOI: 10.1124/mol.112.084368
This article has not been copyedited and formatted. The final version may differ from this version.

Statistical analysis

Quantitative data are expressed as mean ± SD. Data were analyzed by regression analysis, one-way ANOVA, and unpaired Student's t test. $P<0.05$ was considered statistically significant. For nonquantitative data, results are representative of at least 3 independent experiments.

Molecular Pharmacology Fast Forward. Published on March 7, 2013 as DOI: 10.1124/mol.112.084368
This article has not been copyedited and formatted. The final version may differ from this version.

Results

Synthesis and identification of SA1~SA10

To determine the most active compound of SA, we designed and synthesized a series of 1-erucic acyl-4-benzyl piprazine derivatives (SA1~SA10) from synthesized 4-substituted -benzyl piperazine (Supplemental Figure 1A) and its derivatives (Supplemental Figure 1B), named as compounds c1~c10 (Supplemental Table 1). Figure 1A shows the synthesis and determination of the chemical structure and substituents of SA1~SA10. The detailed procedure and the physical constants of the compounds SA1~SA10 are listed in the supplement material (Supplemental Methods, Supplemental Table 2). All structures of SA1~SA10 were identified by elemental analysis, mass spectrometry, ^{1}H nuclear magnetic resonance (^{1}HNMR) and infrared absorption spectra (IR) (Supplemental Tables 3 to 5). The purity of SA1~SA10 was ≥ 98.47 as determined by HPLC (Supplemental Table 6).

SA~SA10 had high DPPH content and hydroxyl free radical scavenging activity

The stable DPPH model is widely used to evaluate antioxidant activity in a relatively short time (Villano et al., 2007). DPPH assay was used to preliminarily screen for antioxidant activity of SA~SA10. The DPPH radical scavenging activities of SA~SA10 were concentration dependent (Supplement Figure 2A), as seen by the high correlation coefficients (R^2 >0.90, p<0.05, linear range 0~150 μM) by logarithmic regression analysis (Supplemental Table 7). SA~SA10 at 150 μM all showed DPPH• scavenging rates > 90%. The EC_{50} value, widely used to measure free radical scavenging activity, when low, indicates high antioxidant activity (Maisuthisakula et al., 2007). The EC_{50} values (Supplemental Table 7) organized by 4 groups (p<0.05): SA<SA10<SA1, SA2, SA8, SA9<SA4, SA6, SA7, SA3, SA5. Thus, SA~SA10 showed high proton-donating ability on DPPH· to form stable DPPH molecules.

Hydroxyl radicals are the major active oxygen species causing lipid peroxidation and enormous biological damage. The hydroxyl radical scavenging activities of SA~SA10 were

Molecular Pharmacology Fast Forward. Published on March 7, 2013 as DOI: 10.1124/mol.112.084368
This article has not been copyedited and formatted. The final version may differ from this version.

also concentration dependent (Supplemental Figure 2B), as seen by the high correlation coefficients (R^2>0.90, p<0.05, linear range 79.43~602.56 μM) (Supplemental Table 8). The EC_{50} values allowed for dividing the derivatives by 7 groups: SA6<SA10<SA4, SA5, SA7<SA1, SA8, SA9<SA3<SA<SA2. Thus, SA~SA10 showed strong activity to inhibit the generation of hydroxyl radicals from the fenton reaction.

Effect of SA~SA10 on the inhibition of croton oil-induced ear edema in mice

To screen the anti-inflammatory properties of the compounds SA to SA10 *in vivo*, we created a mouse model of croton oil-induced edema in ears. Except for SA and SA7, most SAs at 100 or 200 mg·kg^{-1} had effective anti-inflammatory activity (Table 1). Compared with the non-steroidal anti-inflammatory drug ibuprofen, compounds SA9, SA6, SA8, SA1 and SA4 showed higher anti-inflammatory ability, with SA9 having the strongest inhibitory activity at 200 mg·kg^{-1} (45.65% inhibition). Figure 1B shows the chemical structure of SA9.

Effect of SA1~SA10 on TNF-α–induced pre-inflammatory reaction in ECs

To explore the mechanism of the anti-inflammatory ability of SA1~SA10, cultured HUVECs were treated with 10 ng·ml^{-1} TNF-α and 1 μM of each SA derivative. The TNF-α–induced upregulation of ICAM-1 was significantly attenuated by SA3~SA8, SA9 and SA10 (Fig. 2A). Of note, only SA6, and especially SA9, significantly decreased the expression of VCAM-1 with TNF-α treatment (Fig. 2B). In contrast, no SA derivatives had an effect on the regulation of COX-2 (Fig. 2C). At concentrations < 50 μM, SA1~SA10 had little effect on cell survival and did not cause cytotoxicity in HUVECs, as analyzed by MTT assay (Supplemental Figure 2C). The effect of SA9 on inhibiting the expression of ICAM-1 and VCAM-1 was further confirmed at the protein level (Fig. 3A). Thus, the SA derivatives, especially SA9, possessed anti-inflammatory abilities, at least in part, by inhibiting the expression of ICAM-1 and VCAM-1 in ECs. An antioxidant NAC was reported to efficiently

Molecular Pharmacology Fast Forward. Published on March 7, 2013 as DOI: 10.1124/mol.112.084368
This article has not been copyedited and formatted. The final version may differ from this version.

reduce the expression of adhesion molecules in ECs (Faruqi et al., 1997). In this study, we used NAC as a positive control (Fig. 3A), the similar inhibitory effect of SA9 and NAC on TNF-α-induced VCAM-1 and ICAM-1 expression was observed.

SA9 attenuated TNF-α–induced adhesion of THP-1 cells to ECs

Because the expression of adhesion molecules on ECs is a prerequisite for adhesion of leukocytes, we investigated the effect of SA9 on TNF-α-induced THP-1 cell adhesion to HUVECs. Untreated or PMA-activated THP-1 cells were used in the monocyte binding assay to indicate the function of VCAM-1 and ICAM-1. Pretreating HUVECs with 1 μM SA9 significantly reduced both ICAM-1– and VCAM-1–mediated monocyte adhesion induced by TNF-α (Fig. 3B and 3C).

SA9 inhibited inflammation-induced oxidative stress in ECs

To further explore the mechanism by which SA9 exerted its anti-inflammatory effect, we measured TNF-α–induced oxidative stress by superoxide anion generation and ROS level in HUVECs by DHE and DCFH-DA staining, respectively. The antioxidants NAC and DPI were served as the positive control. Exposure to 10 $ng \cdot ml^{-1}$ TNF-α increased superoxide anion generation (DHE in red) and ROS levels (DCFH-DA in green) in HUVECs (Fig. 4A and 4B). However, pretreatment with NAC, DPI and SA9 showed similar effect to prevent the increased oxidative stress in ECs. To study the anti-oxidant effects of SA9 *in vivo*, we measured mouse ear edema in a croton oil-induced mouse model. Croton oil induced blood-vessel dilation, congestion, thickness of mouse ear pieces and infusion of inflammatory cells (Fig. 4C); all were significantly inhibited by SA9. The superoxide anion level and generation of ROS induced by proinflammatory edema were significantly reduced by SA9 (Fig. 4D and 4E).

The anti-inflammatory effects of SA9 was through inhibiting of NF-κB activation

As demonstrated above, SA9 exerted its anti-inflammatory effect by inhibiting

Molecular Pharmacology Fast Forward. Published on March 7, 2013 as DOI: 10.1124/mol.112.084368
This article has not been copyedited and formatted. The final version may differ from this version.

TNF-α–induced oxidative stress and the expression of cell adhesion molecules but not COX-2. Since upregulation of cell adhesion molecules and activation of NF-κB can be induced by TNF-α (Paik et al., 2002), we next studied the involvement of NF-κB in the anti-inflammatory effects of SA9 in ECs. The transfection results in Figure 5A revealed that treatment of TNF-α could activate NF-κB-luc in ECs, which was largely attenuated by SA9 pretreatment. In addition, immunofluorescence analysis revealed that the nuclear translocation of p65, a subunit of NF-κB and marker of its activation, was significantly inhibited by SA9 (Fig. 5B). Furthermore, western blot results showed that with SA9 pretreatment, the phosphorylation of IκB was significantly inhibited. AP-1 is another redox-sensitive transcriptional factor, and the phosphorylation of JNK and ERK upstream of AP-1 activation. Therefore, we also detected the phosphorylation of JNK and ERK and found that phosphorylation of both JNK and ERK was increased by TNF-α, which could be reduced by SA9 to a certain degree (Fig. 5C). Thus, the anti-inflammatory effects of SA9 were by inhibition of NF-κB, but the involvement of AP-1 could not be excluded.

SA9 inhibited the LPS-induced expression of ICAM-1 in mouse aortic intima

To investigate whether SA9 possesses anti-inflammatory effects *in vivo*, we examined LPS-induced expression of ICAM-1 in the aortic endothelium of C57 mice. *En face* immunofluorescence staining showed the expression of ICAM-1 significantly increased in the aortic endothelium when animals were injected LPS to induce a systemic inflammation; the LPS-mediated upregulation of ICAM-1 was significantly attenuated with SA9 administration (Fig. 6). Thus, SA9 had an anti-inflammatory effect by inhibiting the expression of adhesion molecules in vascular endothelium *in vitro* and *in vivo*.

Molecular Pharmacology Fast Forward. Published on March 7, 2013 as DOI: 10.1124/mol.112.084368
This article has not been copyedited and formatted. The final version may differ from this version.

Discussion

SA is a phenylpropanoid compound found in natural herbs and high-bran cereals. It was reported to have moderate antioxidant and anti-inflammatory efficacy (Galano et al., 2011; Kwak et al., 2013; Yun et al., 2008). To improve the antioxidant and anti-inflammatory properties and capitalize on other pharmacological functions of SA, we designed and synthesized 10 SA derivatives by varying the substitution of methyl, methoxy and chloro groups at ortho, meta, and para positions of the phenyl ring. All 10 derivatives showed certain antioxidant activities in a cell-free system, but when tested on cultured cells, SA9 showed higher free radical scavenge activities and stronger inhibitory effects on TNF-α–induced upregulation of adhesion molecules in ECs. Furthermore, SA9 inhibited the monocyte/macrophage adhesion to ECs, and the LPS-induced expression of ICAM-1 in mouse aortic intima. The mechanism was by inhibiting oxidative stress and NF-κB activation in ECs.

Preliminary screening of the anti-oxidant and anti-inflammatory ability of the 10 SA derivatives involved investigating scavenging hydroxyl radicals and DPPH· in cell-free system, expression of adhesion molecules in cultured ECs, and croton oil-induced ear edema in mouse model. Although almost all compounds could scavenge hydroxyl radicals and DPPH· and possessed topical anti-inflammatory properties and excellent biocompatibility, SA9 had stronger antioxidant and anti-inflammatory activity in ECs and animal models.

The fat-soluble and site of substitution on benzyl are important factors affecting antioxidant and anti-inflammatory activity. Chlorine atoms and the meta-substituted position increased the activity of the compounds. Theoretically, a compound with high fat solubilty has better activity. Indeed, the structure of SA9 is the meta-substitution of the benzene ring by the chlorine atom. Thus, SA9 should have efficient anti-oxidation activity, which we

confirmed.

Oxidative stress has long been recognized an important contributor to cardiovascular disease. The production of ROS (free radicals and peroxides), is a particularly detrimental aspect of oxidative stress. Numerous clinical studies showed that increased vascular oxidative stress is strongly associated with cardiovascular events in patients with coronary artery disease (Heitzer et al., 2001). Here, we found that SA9 has ROS scavenger property and could efficiently reduce superoxide anions in ECs. Additional results indicated that SA9 has strong anti-oxidant activity and protects ECs against activation and injury by ROS. Inflammatory status is a risk factor of cardiovascular disease. The expression of cell adhesion molecules, such as VCAM-1 and ICAM-1, mediates monocyte/macrophage adhesion and the consequent processes in initiating atherogenesis (Trerotola et al., 2010). We found that SA9 could significantly inhibit the TNF-α–induced ROS generation, upregulation of ICAM-1 and VCAM-1 in ECs and blocked monocyte adhesion to ECs, similar as the effect of NAC and DPI, well-known antioxidants. It was reported that NAC suppressed TNF-α-stimulated expression of adhesion molecules by inhibiting ROS and NF-κB activity. (Sakurada et al., 1996; Zafarullah et al., 2003). In addition, our preclinical animal model confirmed the anti-inflammatory properties of SA9 in inhibiting the expression of ICAM-1 in the aortic endothelium. Our results are supported by numerous studies showing that reducing intracellular ROS production could inhibit monocyte adhesiveness to ECs (Lin et al., 2005; Paine et al., 2010).

NF-κB, a redox-sensitive transcription factor, could be activated by oxidative stress and is involved in proinflammatory cytokine production (Pueyo et al., 2000). Therefore, we proposed that the anti-inflammatory effects of SA9 were based on the inhibition of NF-κB activation. SA9 potently suppressed TNF-α–mediated activation of NF-κB, and the nuclear

translocation of p65, a subunit of NF-κB, in HUVECs. Thus, the mechanism of the anti-inflammatory effects of SA9 depended on the inhibition of ROS and NF-κB. However, SA9 did not prevent the TNF-α–induced upregulation of COX-2. Regulation of COX-2 by TNF-α was previously found mediated by both MAPK and NF-κB (Paik et al., 2002). The regulation of COX-2 by MAPK and NF-κB are by separate signaling pathways, and p38 MAPK but not NF-κB participates in the regulation of COX-2 mRNA stability (Singer et al., 2003). We found that SA9 mainly inhibited TNF-α-induced the phosphorylation of IKB but also attenuated phosphorylation of JNK and ERK to a certain degree, which suggests the involvement of the AP-1 pathway (cJun/c-Fos). Our results also indicate the induction of COX-2 and VCAM-1/ICAM-1 by cytokines via different mechanisms.

In conclusion, we demonstrated that SA9, a new SA derivative, could efficiently prevent endothelial oxidative stress *in vitro* and *in vivo*. In addition, SA9 could inhibit the TNF-α–induced NF-κB activation and the expression of cell adhesion molecules, for a potential endothelial protective effect. SA9 may provide a new therapeutical approach for preventing endothelial activation in cardiovascular disorders.

Molecular Pharmacology Fast Forward. Published on March 7, 2013 as DOI: 10.1124/mol.112.084368
This article has not been copyedited and formatted. The final version may differ from this version.

Authorship Contributions

Participated in research design: Zhu, Zheng and Zeng

Conducted experiments: Zeng, Fu, Su, Sun, Zhang and Hou

Contributed new reagents or analytical tools: Zeng, Fu, Su, Sun, Zhang and Hou

Performed data analysis: Zeng, Fu, Su, Sun, Zhang, and Zhu

Wrote or contributed to the writing of the manuscript: Zeng, Fu, Sun and Zhu

Molecular Pharmacology Fast Forward. Published on March 7, 2013 as DOI: 10.1124/mol.112.084368
This article has not been copyedited and formatted. The final version may differ from this version.

References

Alom-Ruiz SP, Anilkumar N and Shah AM (2008) Reactive oxygen species and endothelial activation. *Antioxid Redox Signal* **10**(6):1089-1100.

Anderson TJ (1999) Assessment and treatment of endothelial dysfunction in humans. *J Am Coll Cardiol* **34**(3):631-638.

Bonetti PO, Lerman LO and Lerman A (2003) Endothelial dysfunction: a marker of atherosclerotic risk. *Arterioscler Thromb Vasc Biol* **23**(2):168-175.

Borel JC, Roux-Lombard P, Tamisier R, Arnaud C, Monneret D, Arnol N, Baguet JP, Levy P and Pepin JL (2009) Endothelial dysfunction and specific inflammation in obesity hypoventilation syndrome. *PLoS One* **4**(8):e6733.

Butcher EC (1991) Leukocyte-endothelial cell recognition: three (or more) steps to specificity and diversity. *Cell* **67**(6):1033-1036.

Conforti A, Caliceti P, Sartore L, Schiavon O, Veronese F and Velo GP (1991) Anti-inflammatory activity of monomethoxypolyethylene glycol superoxide dismutase on adjuvant arthritis in rats. *Pharmacol Res* **23**(1):51-56.

Corda S, Laplace C, Vicaut E and Duranteau J (2001) Rapid reactive oxygen species production by mitochondria in endothelial cells exposed to tumor necrosis factor-alpha is mediated by ceramide. *Am J Respir Cell Mol Biol* **24**(6):762-768.

Dang H, Liu Y, Pang W, Li C, Wang N, Shyy JY and Zhu Y (2009) Suppression of 2,3-oxidosqualene cyclase by high fat diet contributes to liver X receptor-alpha-mediated improvement of hepatic lipid profile. *J Biol Chem* **284**(10):6218-6226.

Davignon J and Ganz P (2004) Role of endothelial dysfunction in atherosclerosis. *Circulation* **109**(23 Suppl 1):III27-32.

Faruqi RM, Poptic EJ, Faruqi TR, De La Motte C and DiCorleto PE (1997) Distinct mechanisms for N-acetylcysteine inhibition of cytokine-induced E-selectin and VCAM-1 expression. *Am J Physiol* **273**(2 Pt 2):H817-826.

Fenster BE, Tsao PS and Rockson SG (2003) Endothelial dysfunction: clinical strategies for treating oxidant stress. *Am Heart J* **146**(2):218-226.

Fu C, He J, Li C, b JY-JS and Zhu Y (2010a) Cholesterol increases adhesion of monocytes to endothelium by moving adhesion molecules out of caveolae. *Biochim Biophys Acta* **1801**(7):702-710.

Fu Y, Hou Y, Fu C, Gu M, Li C, Kong W, Wang X, Shyy JY and Zhu Y (2011) A novel mechanism of gamma/delta T-lymphocyte and endothelial activation by shear stress: the role of ecto-ATP synthase beta chain. *Circ Res* **108**(4):410-417.

Galano A, Francisco-Marquez M and Alvarez-Idaboy JR (2011) Mechanism and kinetics studies on the antioxidant activity of sinapinic acid. *Phys Chem Chem Phys* **13**(23):11199-11205.

Garrean S, Gao XP, Brovkovych V, Shimizu J, Zhao YY, Vogel SM and Malik AB (2006) Caveolin-1 regulates NF-kappaB activation and lung inflammatory response to sepsis induced by lipopolysaccharide. *J Immunol* **177**(7):4853-4860.

Heitzer T, Schlinzig T, Krohn K, Meinertz T and Munzel T (2001) Endothelial dysfunction, oxidative stress, and risk of cardiovascular events in patients with coronary artery disease. *Circulation* **104**(22):2673-2678.

Kim YM, Kim MY, Kim HJ, Roh GS, Ko GH, Seo HG, Lee JH and Chang KC (2011) Compound C independent of AMPK inhibits ICAM-1 and VCAM-1 expression in inflammatory stimulants-activated endothelial cells in vitro and in vivo. *Atherosclerosis* **219**(1):57-64.

Kwak SY, Yang JK, Choi HR, Park KC, Kim YB and Lee YS (2013) Synthesis and dual biological effects of

hydroxycinnamoyl phenylalanyl/prolyl hydroxamic acid derivatives as tyrosinase inhibitor and antioxidant. *Bioorg Med Chem Lett* **23**(4):1136-1142.

Lefevre J, Michaud SE, Haddad P, Dussault S, Menard C, Groleau J, Turgeon J and Rivard A (2007) Moderate consumption of red wine (cabernet sauvignon) improves ischemia-induced neovascularization in ApoE-deficient mice: effect on endothelial progenitor cells and nitric oxide. *FASEB J* **21**(14):3845-3852.

Lin SJ, Shyue SK, Hung YY, Chen YH, Ku HH, Chen JW, Tam KB and Chen YL (2005) Superoxide dismutase inhibits the expression of vascular cell adhesion molecule-1 and intracellular cell adhesion molecule-1 induced by tumor necrosis factor-alpha in human endothelial cells through the JNK/p38 pathways. *Arterioscler Thromb Vasc Biol* **25**(2):334-340.

Lum H and Roebuck KA (2001) Oxidant stress and endothelial cell dysfunction. *Am J Physiol Cell Physiol* **280**(4):C719-741.

Maisuthisakula P, Suttajitb M and Pongsawatmanit R (2007) Assessment of phenolic content and free radical-scavenging capacity of some Thai indigenous plants. . *Food Chem* **100**(4):1409–1418.

Ming J, Yaxin C, Jinrong L and Hui Z (1996) 1,10-Phenanthroline-Fe2+ Oxidative Assay of Hydroxyl Radical Produced by H2O2/Fe2+. *Progress in Biochemistry and Biophysics* **23**(6):553-555.

Munzel T, Gori T, Bruno RM and Taddei S (2010) Is oxidative stress a therapeutic target in cardiovascular disease? *Eur Heart J* **31**(22):2741-2748.

Olajide OA, Makinde JM, Okpako DT and Awe SO (2000) Studies on the anti-inflammatory and related pharmacological properties of the aqueous extract of Bridelia ferruginea stem bark. *J Ethnopharmacol* **71**(1-2):153-160.

Paik J, Lee JY and Hwang D (2002) Signaling pathways for TNFa-induced COX-2 expression: mediation through MAP kinases and NFkB, and inhibition by certain nonsteroidal anti-inflammatory drugs. *Adv Exp Med Biol* **507**:503-508.

Paine A, Eiz-Vesper B, Blasczyk R and Immenschuh S (2010) Signaling to heme oxygenase-1 and its anti-inflammatory therapeutic potential. *Biochem Pharmacol* **80**(12):1895-1903.

Pober JS, Min W and Bradley JR (2009) Mechanisms of endothelial dysfunction, injury, and death. *Annu Rev Pathol* **4**:71-95.

Pratico D (2005) Antioxidants and endothelium protection. *Atherosclerosis* **181**(2):215-224.

Pueyo ME, Gonzalez W, Nicoletti A, Savoie F, Arnal JF and Michel JB (2000) Angiotensin II stimulates endothelial vascular cell adhesion molecule-1 via nuclear factor-kappaB activation induced by intracellular oxidative stress. *Arterioscler Thromb Vasc Biol* **20**(3):645-651.

Sakurada S, Kato T and Okamoto T (1996) Induction of cytokines and ICAM-1 by proinflammatory cytokines in primary rheumatoid synovial fibroblasts and inhibition by N-acetyl-L-cysteine and aspirin. *Int Immunol* **8**(10):1483-1493.

Shindel AW, Kishore S and Lue TF (2008) Drugs designed to improve endothelial function: effects on erectile dysfunction. *Curr Pharm Des* **14**(35):3758-3767.

Singer CA, Baker KJ, McCaffrey A, AuCoin DP, Dechert MA and Gerthoffer WT (2003) p38 MAPK and NF-kappaB mediate COX-2 expression in human airway myocytes. *Am J Physiol Lung Cell Mol Physiol* **285**(5):L1087-1098.

Trerotola M, Guerra E and Alberti S (2010) Letter to the editor: efficacy and safety of anti-Trop antibodies, R. Cubas, M. Li, C. Chen and Q. Yao, Biochim Biophys Acta 1796 (2009) 309-1. *Biochim Biophys Acta* **1805**(2):119-120; author reply 121-112.

Verna L, Ganda C and Stemerman MB (2006) In vivo low-density lipoprotein exposure induces intercellular adhesion molecule-1 and vascular cell adhesion molecule-1 correlated with activator protein-1 expression.

Arterioscler Thromb Vasc Biol **26**(6):1344-1349.

Versari D, Daghini E, Virdis A, Ghiadoni L and Taddei S (2009) Endothelial dysfunction as a target for prevention of cardiovascular disease. *Diabetes Care* **32 Suppl 2**:S314-321.

Villano D, Fernandez-Pachon MS, Moya ML, Troncoso AM and Garcia-Parrilla MC (2007) Radical scavenging ability of polyphenolic compounds towards DPPH free radical. *Talanta* **71**(1):230-235.

Wagener FA, Feldman E, de Witte T and Abraham NG (1997) Heme induces the expression of adhesion molecules ICAM-1, VCAM-1, and E selectin in vascular endothelial cells. *Proc Soc Exp Biol Med* **216**(3):456-463.

Yun KJ, Koh DJ, Kim SH, Park SJ, Ryu JH, Kim DG, Lee JY and Lee KT (2008) Anti-inflammatory effects of sinapic acid through the suppression of inducible nitric oxide synthase, cyclooxygase-2, and proinflammatory cytokines expressions via nuclear factor-kappaB inactivation. *J Agric Food Chem* **56**(21):10265-10272.

Zafarullah M, Li WQ, Sylvester J and Ahmad M (2003) Molecular mechanisms of N-acetylcysteine actions. *Cell Mol Life Sci* **60**(1):6-20.

Zhang D, Ai D, Tanaka H, Hammock BD and Zhu Y (2010) DNA methylation of the promoter of soluble epoxide hydrolase silences its expression by an SP-1-dependent mechanism. *Biochim Biophys Acta* **1799**(9):659-667.

Zhang DH, Marconi A, Xu LM, Yang CX, Sun GW, Feng XL, Ling CQ, Qin WZ, Uzan G and d'Alessio P (2006) Tripterine inhibits the expression of adhesion molecules in activated endothelial cells. *J Leukoc Biol* **80**(2):309-319.

Zhu M, Fu Y, Hou Y, Wang N, Guan Y, Tang C, Shyy JY and Zhu Y (2008) Laminar shear stress regulates liver X receptor in vascular endothelial cells. *Arterioscler Thromb Vasc Biol* **28**(3):527-533.

Molecular Pharmacology Fast Forward. Published on March 7, 2013 as DOI: 10.1124/mol.112.084368
This article has not been copyedited and formatted. The final version may differ from this version.

Footnote

This work was supported in part by grants from the Major National Basic Research Grant of China [2010CB912504]; the National Natural Science Foundation of China [30971063, 81130002]; the Team Project of the Natural Science Foundation of the Guangdong Province [9351503102000001] and the Project of the Natural Science Foundation of Guangdong Province of China [10151503102000048].

Molecular Pharmacology Fast Forward. Published on March 7, 2013 as DOI: 10.1124/mol.112.084368
This article has not been copyedited and formatted. The final version may differ from this version.

Conflict-of-interest

We have applied for a China patent for the synthesis and application of the compounds of SA1~SA10 used in this study (application no. 201010112900.7, publication no. 101787002). No other conflicts of interest.

Molecular Pharmacology Fast Forward. Published on March 7, 2013 as DOI: 10.1124/mol.112.084368
This article has not been copyedited and formatted. The final version may differ from this version.

Figure Legends

Figure. 1. Synthesis, chemical structures, and substituents of sinapic acid derivatives (SA1~SA10). (A) Synthesis of SA (a), acetyl sinapic acid (b), acetyl sinapic chloride (c), piperazine dihydrochloride monohydrate (d), and N-benzyl piperazine hydrochloride (e), and synthesis of SA1~SA10. (B) Structure of SA9, 1-acetyl-sinapic acyl-4-(3'-Chlorine-) benzylpiperazine.

Figure 2. Effect of SA1~SA10 on TNF-α–inhibition of intracellular ICAM-1, VCAM-1 and COX-2 in HUVECs. HUVECs were pretreated with 10 ng·ml^{-1} TNF-α and 1 μM SA1 ~ SA10 for 6 hr. RT-PCR analysis of mRNA levels of human ICAM-1 (A), VCAM-1 (B), and cyclooxygenase 2 (COX-2) (C). GAPDH cDNA was an internal control. Data are mean± SD of mRNA relative to that of GAPDH from 3 independent experiments. $^{*}p < 0.05$ vs. control (Ctrl); $^{\#}p < 0.05$; $^{\#\#}p < 0.01$ vs. TNF-α.

Figure 3. The inhibitory effect of SA9 on TNFα-induced adhesion molecules and monocyte adhesion to ECs. (A) HUVECs were pretreated with 1 μM SA9 or 1mM NAC for 30 min, and then with 10 ng·ml^{-1} TNF-α for 8 hr. Whole cells were lysed, and ICAM-1 and VCAM-1 protein were measured by western blot analysis. β-actin was a loading control. Data are mean±SD of the protein normalized to that of β-actin from 3 independent experiments. $^{*}p < 0.05$ vs. control (Ctrl); $^{\#}p < 0.05$ vs. TNF-α. (B) HUVECs were pretreated with 1 μM SA9 for 30 min, then treated with 10 ng·ml^{-1} TNF-α for 8 hr. (C) THP-1 cells were stimulated with or without PMA and then labeled with fluorescence dye. Cell adhesion assay was performed. Representative results and quantitative results show fold change in cell adhesion as compared with untreated controls. Data are the mean±SD of 4 independent

Molecular Pharmacology Fast Forward. Published on March 7, 2013 as DOI: 10.1124/mol.112.084368
This article has not been copyedited and formatted. The final version may differ from this version.

experiments, each performed in triplicate. $^{*}p < 0.05$; $^{**}p < 0.01$.

Figure 4. SA9 inhibited inflammation-induced oxidative stress *in vitro* and *in vivo*. (A and B) HUVECs were pretreated with 1 mM NAC, 20 μM DPI or 1 μM SA9 for 30 min, then with 10 ng·ml^{-1} TNF-α for 30 min in the DCFH-DA assay and 20 min in the DHE assay. Quantification of DCFH-DA and DHE images was from 4 different experiments by use of a fluorescence microplate reader (BioTek, Gen5). $^{*}p < 0.05$; $^{**}p < 0.01$ vs. control (Ctrl); $^{\#}p < 0.05$; $^{\#\#}p < 0.01$ vs. TNF-α. (C-E) Croton oil (1%, 50 μL per mouse) was applied on the right ear pinna of BALB/c mice, and the left pinna was used as control. The mice were euthanized 4 hr after croton oil was applied, then ears were removed. (C) Cross-sections of the ears with HE staining (magnification: 100× and 400×) and quantification. Arrows indicated blood vessels dilated and congested, and infiltrated inflammatory cells in the dermis. Superoxide anion level measured by DHE staining (D), and ROS levels measured by DCFH-DA staining (E). Magnification: 400×, Data are mean±SD from 6 mice (right). $^{*}p < 0.05$; $^{**}p < 0.01$.

Figure 5. The anti-inflammatory effects of SA9 was by inhibiting of NF-κB. (A) Hy926 cells were transfected with NF-κB-luc for 24 hr and then treated with 10 ng·ml^{-1} TNF-α and 1 μM SA9 for another 24 hr. β-gal plasmid was co-transfected as a transfection control. Luciferase activities were normalized to that of β-galactosidase. Data are mean ± SD of the relative luciferase activities from 3 independent experiments, each performed in triplicate (*, $p<0.05$). (B) HUVECs were treated with 10 ng·ml^{-1} TNF-α and 1 μM SA9 for 2 hr. NF-κB subunit p65 was stained with rabbit anti-p65 and anti-rabbit FITC-conjugated secondary antibody (green) and Hoechst dye was used for nuclear staining (blue). The images were observed by confocal fluorescence microscopy. Results are representative of 3 separate experiments. (C) HUVECs were pretreated with 10 ng·ml^{-1} TNF-α and 1 μM SA9 for 5 and 30 min. Western blot analysis of protein levels of p-IκB, t-IκB, p-JNK, JNK1, p-ERK and t-ERK. Results are representative of 3 independent experiments. Bar graphs show the band

Molecular Pharmacology Fast Forward. Published on March 7, 2013 as DOI: 10.1124/mol.112.084368
This article has not been copyedited and formatted. The final version may differ from this version.

density ratio of phosphorylated to total protein levels (p-IκB/t-IκB, p-JNK/JNK1 and p-ERK/t-ERK), respectively. $^{**}p< 0.01$ vs. control (Ctrl). $^{\#\#}p< 0.01$ vs. TNF-α.

Figure 6. SA9 inhibited the expression of ICAM-1 on mouse aortic intima induced by LPS *in vivo*. C57B mice were fed 50 mg·kg^{-1} body weight SA9 for 1 hr, then the inflammation was induced by intraperitoneal injection of LPS (10 mg·kg^{-1} body weight) for 8 hr. Sections of aortic endothelial underwent *en face* immunostaining for ICAM-1. The red fluorescent staining indicates surface ICAM-1 immunoreactivity, and blue staining represents nuclear staining by Hoechst 33258. Images are representative of results from 6 mice. Bar graphs show the average density of ICAM-1 relative expression. $^{*}p< 0.05$.

Molecular Pharmacology Fast Forward. Published on March 7, 2013 as DOI: 10.1124/mol.112.084368
This article has not been copyedited and formatted. The final version may differ from this version.

Table 1. Effect of compounds at 100 or 200 mg·kg^{-1} on Croton oil-induced ear edema in mice

Compound	Edema (mg) (100 mg·kg^{-1}) mean±SD, n=8	Edema (mg) (200 mg·kg^{-1}) mean±SD, n=8	Inhibition% (100 mg·kg^{-1})	Inhibition% (200 mg·kg^{-1})
Ctrl	14.08±1.11	14.08±1.11	-	-
Croton oil	19.23±1.36 ^{a*}	19.23±1.36 ^{a*}	-	-
Ibu	13.32±2.83 $^{b\#}$	11.37±4.16 $^{b\#\#}$	21.33	32.86
SA	23.6±3.54 $^{b\,ns}$	20.00±1.72 $^{b\,ns}$	-39.41	-18.14
SA1	14.87±2.38 $^{b\,ns}$	10.88±4.48 $^{b\#\#}$	12.18	35.71
SA2	14.72±2.30 $^{b\,ns}$	14.42±3.93 $^{b\#}$	13.07	14.84
SA3	14.88±2.78 $^{b\,ns}$	14.30±2.58 $^{b\#}$	12.08	15.53
SA4	14.17±3.22 $^{b\,ns}$	11.02±2.68 $^{b\#\#}$	16.32	34.92
SA5	13.13±3.75 $^{b\#}$	11.92±2.35 $^{b\#\#}$	22.42	29.61
SA6	13.22±2.76 $^{b\#}$	9.88±3.90 $^{b\#\#}$	21.93	41.62
SA7	21.93±3.29 $^{b\,ns}$	18.60±2.63 $^{b\,ns}$	-29.56	-9.87
SA8	13.65±2.17 $^{b\#}$	9.90±3.79 $^{b\#\#}$	19.37	41.52
SA9	12.97±3.38 $^{b\#}$	9.20±4.27 $^{b\#\#}$	23.4	45.65
SA10	14.78±3.87 $^{b\,ns}$	13.63±4.52 $^{b\#}$	12.67	19.47

$^{a*}p < 0.05$ vs control. $^{b\#\#}p < 0.01$, $^{b\#}p < 0.05$ vs croton oil. (ANOVA, Newman-Keuls

Molecular Pharmacology Fast Forward. Published on March 7, 2013 as DOI: 10.1124/mol.112.084368
This article has not been copyedited and formatted. The final version may differ from this version.

Multiple Comparison Test); Data are mean ± SD (n = 8) or percentage. ns, not significant.

Fig. 1

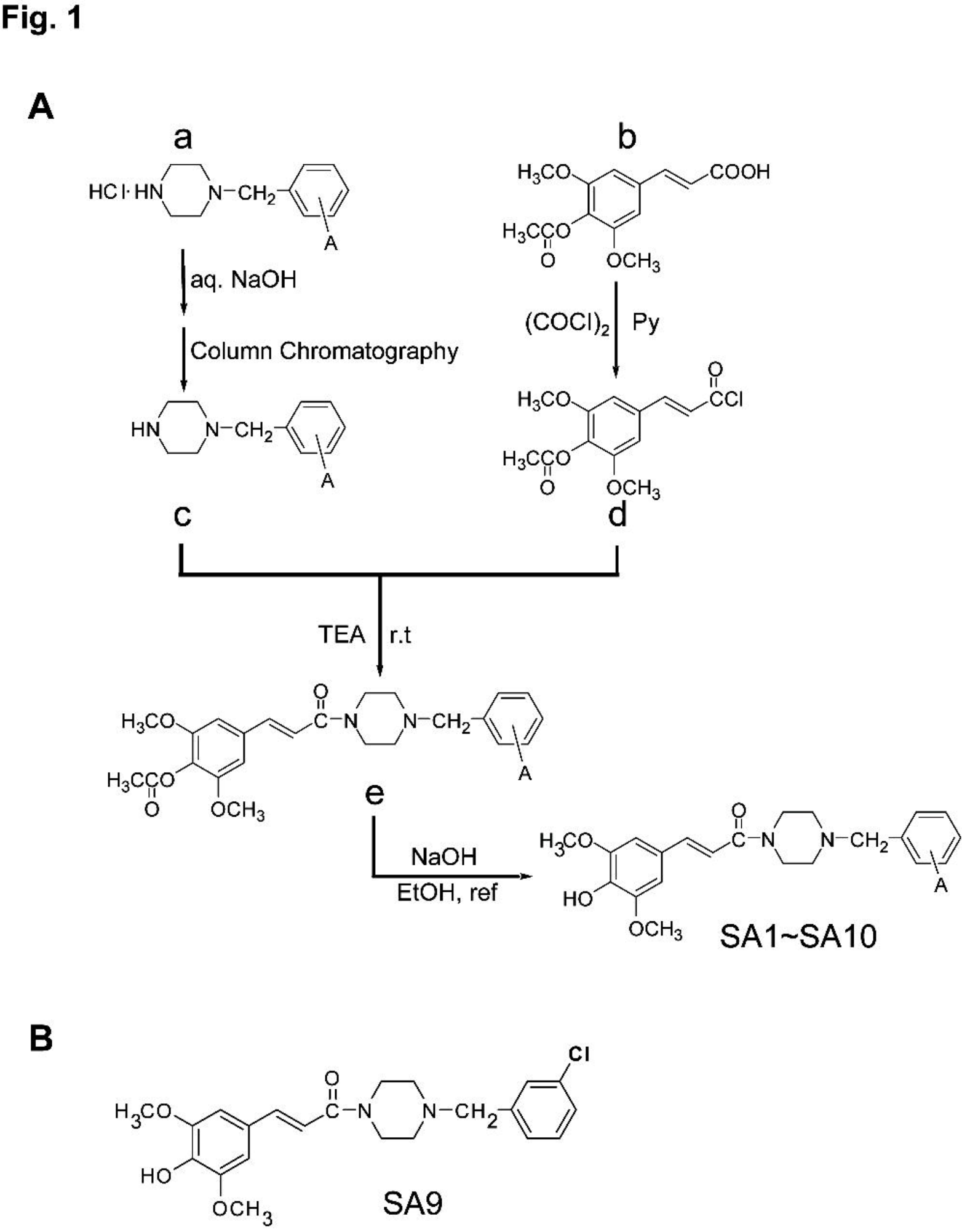
A
a
b
aq. NaOH
Column Chromatography
(COCl)2
Py
c
d
TEA
r.t
e
NaOH
EtOH, ref
SA1~SA10
B
SA9

Fig. 2

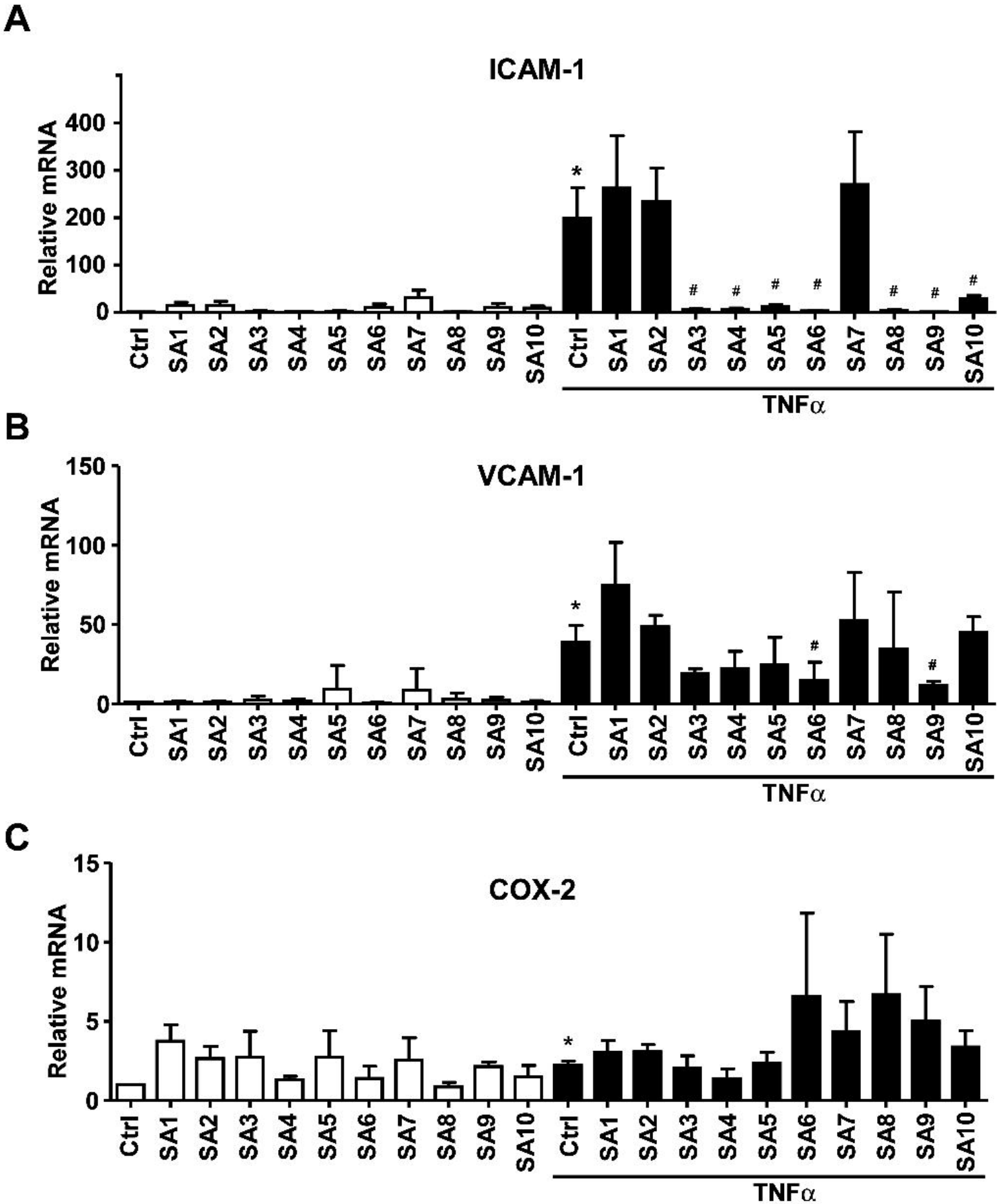
A
ICAM-1
Relative mRNA
400
300
200
100
0
Ctrl
SA1
SA2
SA3
SA4
SA5
SA6
SA7
SA8
SA9
SA10
TNFα
B
VCAM-1
Relative mRNA
150
100
50
0
C
COX-2
Relative mRNA
15
10
5
0

Fig. 3

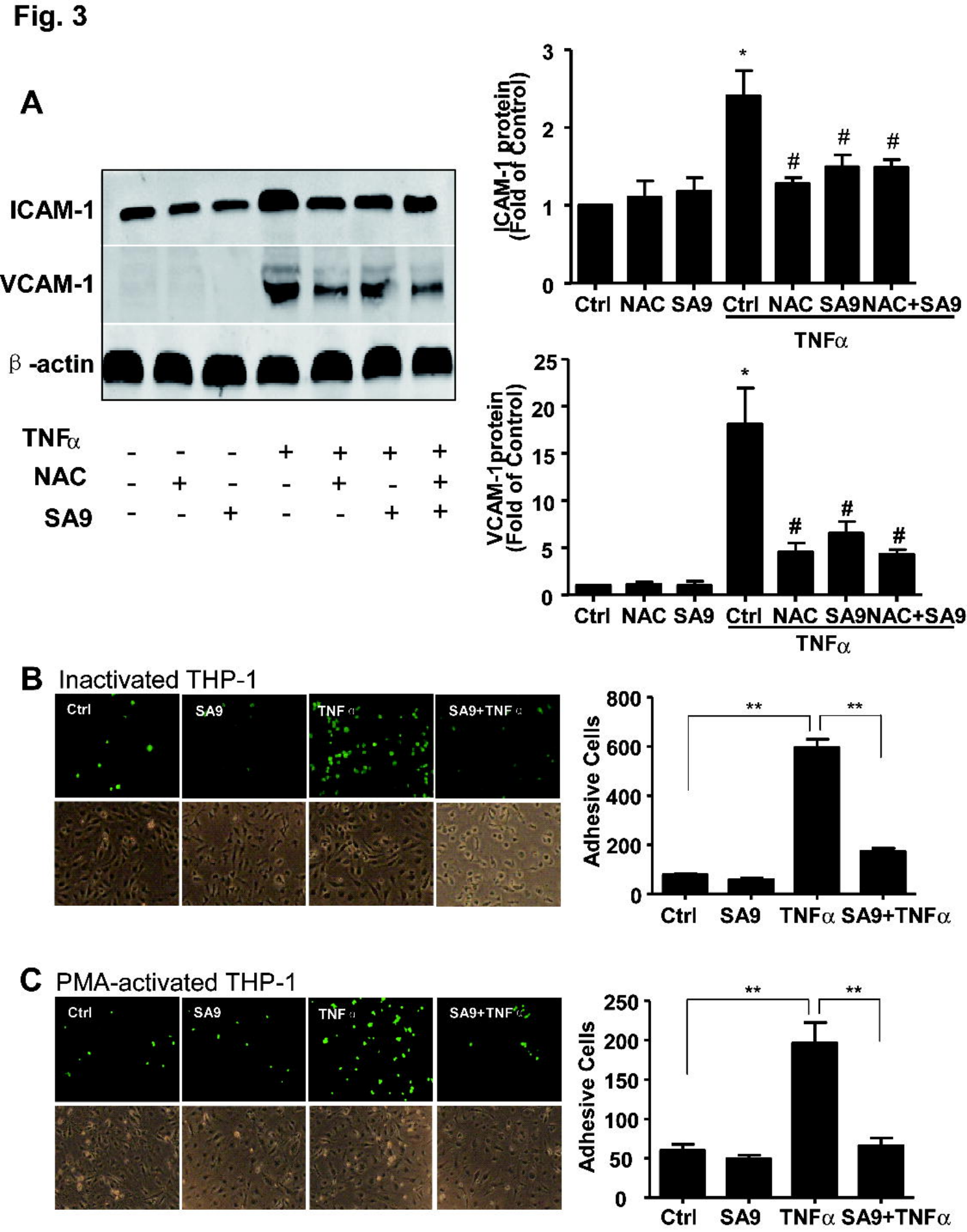
A
ICAM-1
VCAM-1
β -actin
TNFα - - - + + + +
NAC - + - - + - +
SA9 - - + - - + +
ICAM-1 protein (Fold of Control)
Ctrl NAC SA9 Ctrl NAC SA9 NAC+SA9
TNFα
VCAM-1 protein (Fold of Control)
Ctrl NAC SA9 Ctrl NAC SA9 NAC+SA9
TNFα
B Inactivated THP-1
Ctrl
SA9
TNFα
SA9+TNFα
Adhesive Cells
Ctrl SA9 TNFα SA9+TNFα
C PMA-activated THP-1
Ctrl
SA9
TNFα
SA9+TNFα
Adhesive Cells
Ctrl SA9 TNFα SA9+TNFα

Fig. 4

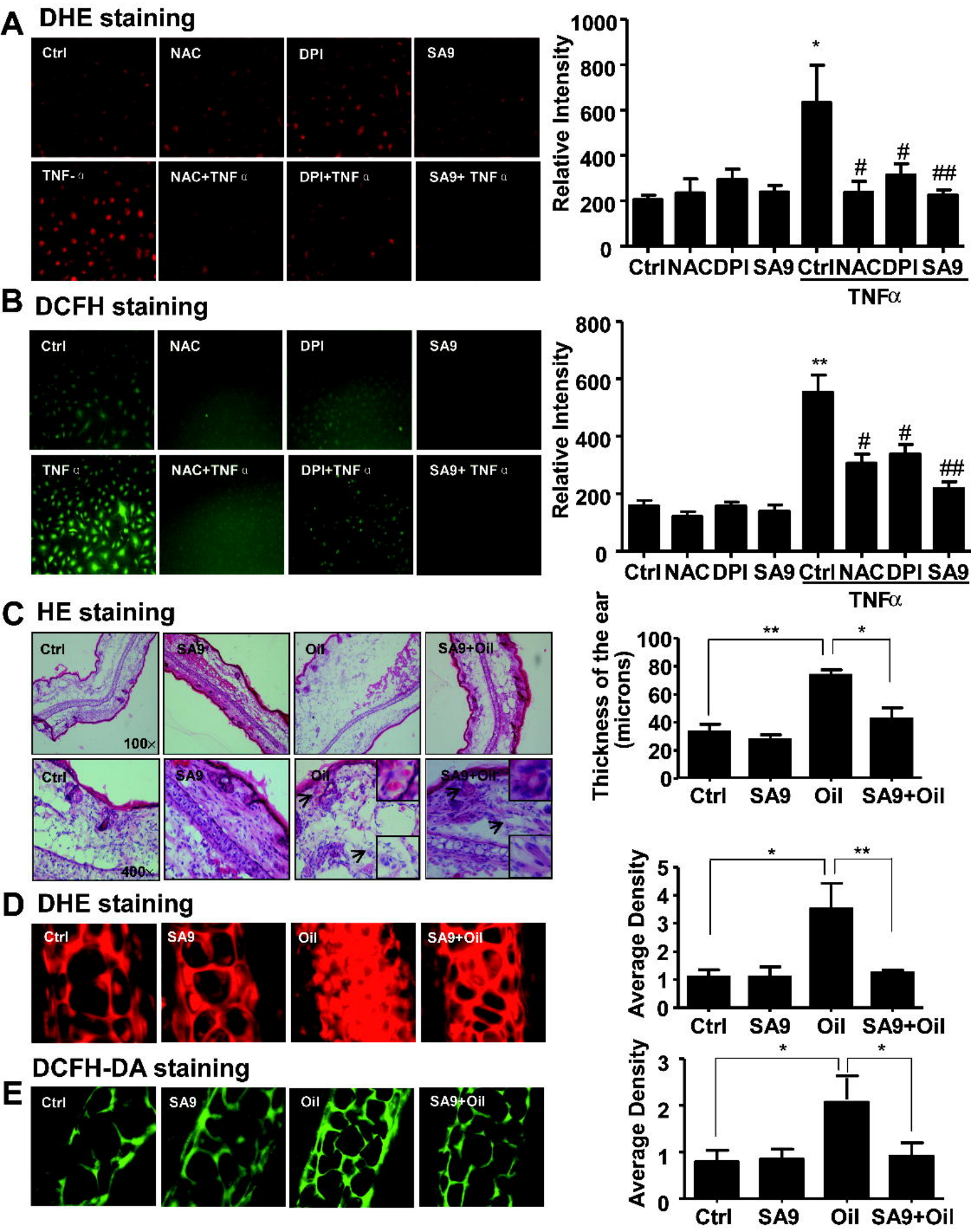
A
DHE staining
Ctrl
NAC
DPI
SA9
TNF-α
NAC+TNF α
DPI+TNF α
SA9+ TNF α
Relative Intensity
1000
800
600
400
200
0
*
#
#
##
Ctrl NAC DPI SA9 Ctrl NAC DPI SA9
TNFα
B
DCFH staining
Ctrl
NAC
DPI
SA9
TNF α
NAC+TNF α
DPI+TNF α
SA9+ TNF α
Relative Intensity
800
600
400
200
0
**
#
#
##
Ctrl NAC DPI SA9 Ctrl NAC DPI SA9
TNFα
C
HE staining
Ctrl
SA9
Oil
SA9+Oil
100×
400×
Thickness of the ear (microns)
100
80
60
40
20
0
**
*
Ctrl SA9 Oil SA9+Oil
D
DHE staining
Ctrl
SA9
Oil
SA9+Oil
Average Density
5
4
3
2
1
0
*
**
Ctrl SA9 Oil SA9+Oil
E
DCFH-DA staining
Ctrl
SA9
Oil
SA9+Oil
Average Density
3
2
1
0
*
*
Ctrl SA9 Oil SA9+Oil

Fig. 5

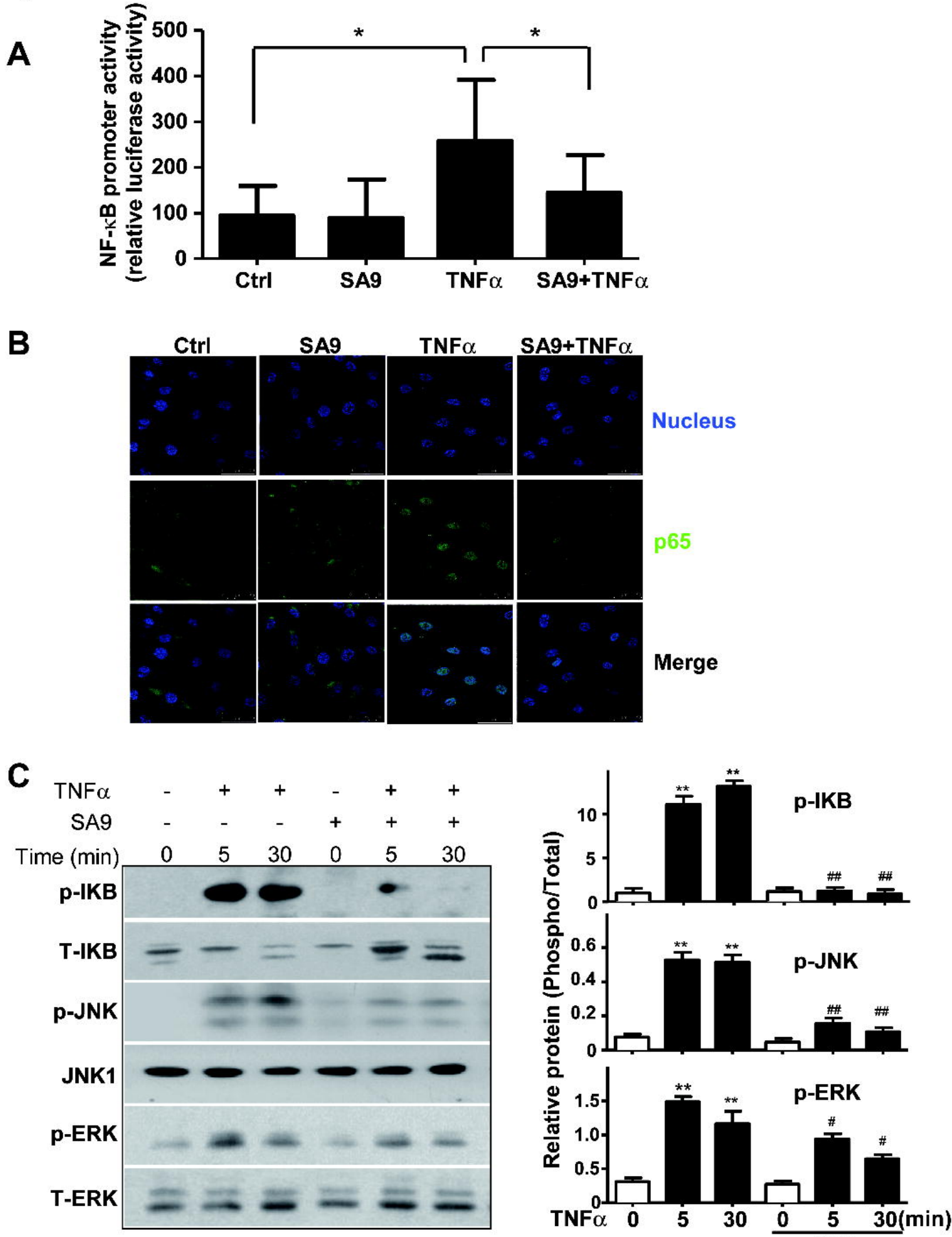
A
NF-κB promoter activity (relative luciferase activity)
500
400
300
200
100
0
*
*
Ctrl
SA9
TNFα
SA9+TNFα
B
Ctrl
SA9
TNFα
SA9+TNFα
Nucleus
p65
Merge
C
TNFα - + + - + +
SA9 - - - + + +
Time (min) 0 5 30 0 5 30
p-IKB
T-IKB
p-JNK
JNK1
p-ERK
T-ERK
Relative protein (Phospho/Total)
p-IKB
p-JNK
p-ERK
**
##
#
TNFα 0 5 30 0 5 30(min)
SA9

Fig. 6

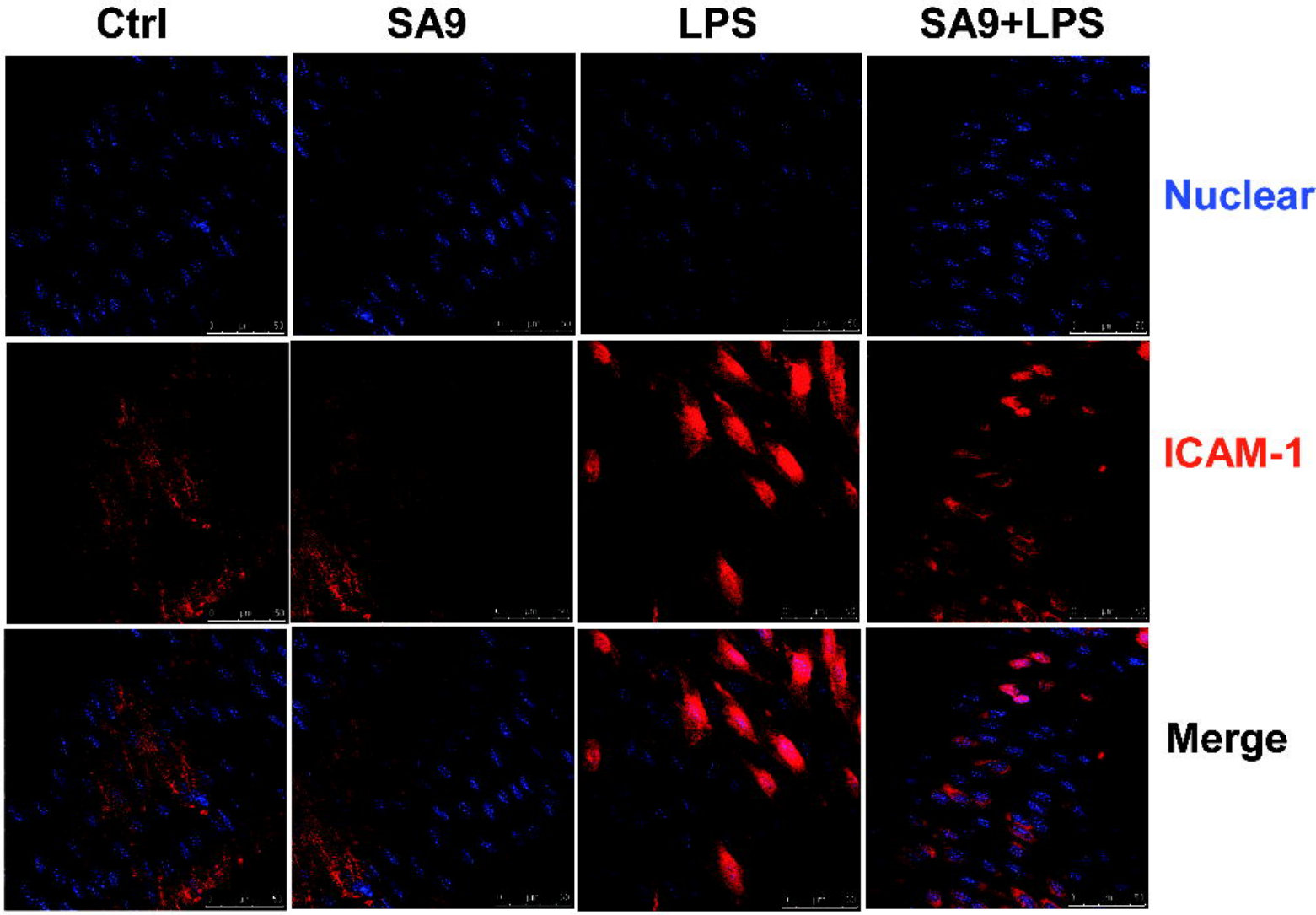
Ctrl
SA9
LPS
SA9+LPS
Nuclear
ICAM-1
Merge

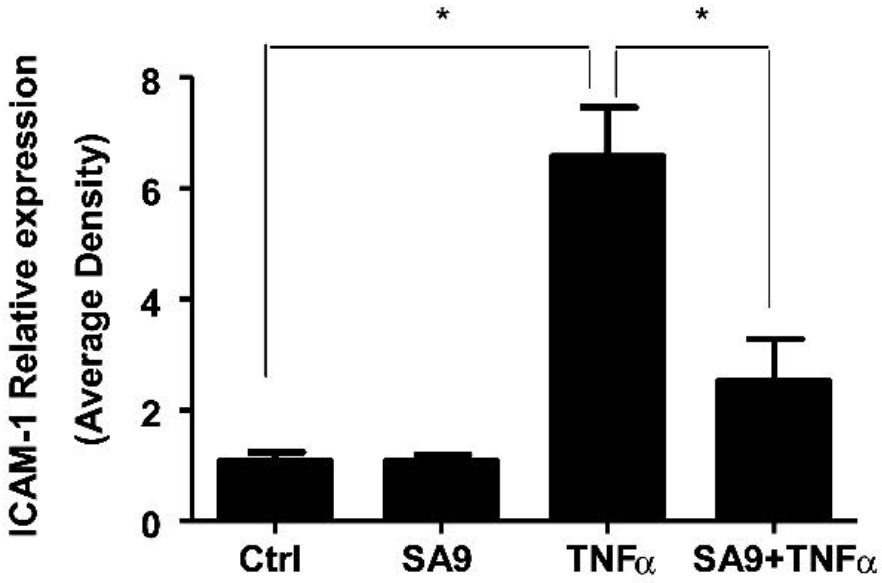
*
*
ICAM-1 Relative expression
(Average Density)
8
6
4
2
0
Ctrl
SA9
TNFα
SA9+TNFα